

## Rapid Screening of Gold Catalysts by Chemiluminescence-Based Array Imaging

Xin Wang, Na Na, Sichun Zhang,\* Yayan Wu, and Xinrong Zhang\*

Department of Chemistry, Key Laboratory of Atomic and Molecular Nanosciences of the Education Ministry, Tsinghua University, Beijing 100084, People's Republic of China

Received January 14, 2007; E-mail: sczhang@chem.tsinghua.edu.cn; xrzhang@chem.tsinghua.edu.cn

Gold catalysts have attracted considerable interests since the extraordinary activity of gold for the oxidation of CO at low temperature was reported.<sup>1–7</sup> Especially, a variety of highly active gold catalysts have been pursued for a series of important industrial reactions.<sup>2,8</sup> Therefore, it has become crucial in the field of catalysis to develop innovative approaches allowing rapid evaluation of the activity by screening a large diversity of catalyst candidates for a specific catalytic reaction. An intensive effort is currently devoted toward the development of high-throughput screening approaches, such as IR thermography,<sup>9</sup> laser-induced fluorescence imaging,<sup>10,11</sup> and resonance-enhanced multiphoton ionization.<sup>12</sup> Although those techniques are very elegant, a simple and straightforward approach should be exploited to achieve rapid screening for catalytic activity of gold catalysts.

The catalytic reaction of some compounds is accompanied by chemiluminescence (CL), which has been studied by many research groups.<sup>13–15</sup> In our previous study, we have also observed the CL emission of many analytes during catalytic reaction on nanomaterials and designed a series of sensors for measuring alcohols, amines, thiols, and other compounds.<sup>16</sup> Moreover, different morphology and components of catalytic nanomaterials led to different CL responses.<sup>16b</sup> We have also concluded that luminescent efficiencies and spectral shapes of the CL depended on the kinds of reactants and catalysts.<sup>16a</sup> Recently, it was found that the CL intensity was correlated with the yield of acetaldehyde from ethanol oxidation over a  $\text{Ce}_{1-x}\text{Zr}_x\text{O}_2$  catalyst.<sup>16c</sup> Those experimental results indicate that the CL is closely related to properties of the reactants and the catalysts. Therefore, it is reasonable to establish a new and rapid approach for evaluating and screening the catalysts based on the CL performance of corresponding catalytic reactions.

In this communication, *the proof of principle* of the CL screening method has been presented by evaluating the catalytic activity of a gold catalyst on the CO conversion as the model. We measured the CL responses of CO oxidation on oxide-supported gold catalysts and correlated the CL features with the catalytic activity for the CO conversion. Moreover, an array was designed for the CL imaging by spotting different gold catalysts on a chip. The brightness of the image is consistent with the corresponding catalytic activities of those catalysts.

A variety of the commercially available oxide supports, including acidic oxide  $\text{SiO}_2$ , basic oxide  $\text{ZnO}$  and  $\text{MgO}$ , and other oxide  $\text{TiO}_2$  and  $\text{ZrO}_2$ , which have been extensively studied for the gold catalysis in converting CO to  $\text{CO}_2$ , were chosen for preparing the supported gold catalysts because these supports displayed different effect on the activity of the gold catalyst.<sup>4</sup> The representative TEM images of these supported gold catalysts prepared with a colloidal deposition method are shown in Figure S1. Size distribution of the gold nanoparticles (NPs) is homogeneous, and the average particle size is in the range of 2–4 nm. It is clear that gold NPs are well dispersed on the surface of oxides, and no obvious aggregation of

gold NPs is observed, indicating that these gold NPs successfully deposited on the supports.

We examined the CL behaviors of catalytic CO oxidation on the surface of various gold catalysts and observed different CL responses. The CL response profiles are displayed in Figure 1, which are comprised of three signals from three replicate injections of CO gas. The maximum CL occurs with  $\text{Au/TiO}_2$ , whereas the minimum one occurs with  $\text{Au/ZnO}$ . Additionally, the CL is enhanced with an increasing amount of CO and reaction temperature (Table S1). The CL spectrum of CO oxidation is obtained, and the mechanism of catalytic CO oxidation is also discussed (see Supporting Information). On the basis of CL intensities, an order can be ranked as  $\text{Au/TiO}_2 > \text{Au/MgO} > \text{Au/SiO}_2 > \text{Au/ZrO}_2 > \text{Au/ZnO}$ .

The catalytic activities of these oxide-supported gold catalysts were also evaluated by gas chromatography (GC), obtaining a typical set of curves for CO conversion as a function of temperature shown in Figure 2.  $T_{100\%}$ , the temperature at which conversion of CO reaches 100%, is chosen to judge the catalytic activities for these gold catalysts. The values of  $T_{100\%}$  are –19, 42, 65, 74, and 84 °C for  $\text{Au/TiO}_2$ ,  $\text{Au/MgO}$ ,  $\text{Au/SiO}_2$ ,  $\text{Au/ZrO}_2$ , and  $\text{Au/ZnO}$ , respectively. A lower  $T_{100\%}$  value indicates a higher catalytic activity. The  $\text{Au/TiO}_2$  has extremely high catalytic activity with a  $T_{100\%}$  value below 0 °C, whereas the  $\text{Au/ZnO}$  catalyst has a relatively lower catalytic activity with a  $T_{100\%}$  value above 80 °C. A comparison of  $T_{100\%}$  corresponding to each oxide-supported gold catalysts is displayed in the inset of Figure 2. On the basis of value of  $T_{100\%}$ , the order of catalytic activity for producing  $\text{CO}_2$  is  $\text{Au/TiO}_2 > \text{Au/MgO} > \text{Au/SiO}_2 > \text{Au/ZrO}_2 > \text{Au/ZnO}$ .

To examine the correlation between CL intensities and CO conversions, we measured the CL responses by passing CO gas through the different gold catalysts at about 160 °C, and at the same time, we collected the corresponding products to measure the CO conversion. As shown in Figure 3A, the correlation coefficient is 0.91, indicating a good correlation between CL intensities and CO conversions. We also took the  $\text{Au/ZnO}$  catalyst as an example to examine the correlation between CL intensities and CO conversions at a series of temperatures and obtained a good correlation (Figure 3B). These results are easily understood because the catalytic reaction is carried out according to the following formula<sup>13,14</sup>



and CL emission is attributed to the decay of the excited state  $\text{CO}_2^*$  to the ground state  $\text{CO}_2$ . Moreover, the CL intensity is proportional to the yield of  $\text{CO}_2$  molecules. The good correlation indicates that the CL intensity could be applied for the screening of the catalytic activity.

To demonstrate the potential of the CL-based approach for rapid and parallel screening of catalytic activity, we designed an array

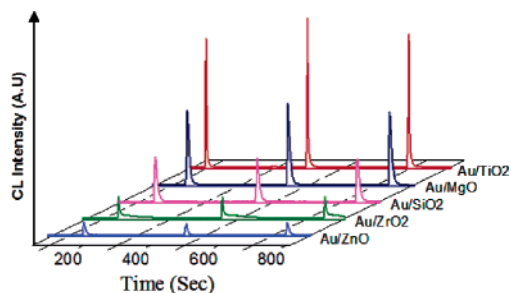


**Figure 1.** Typical CL responses of catalytic CO oxidation on the surface of different oxide-supported gold catalysts. Detection conditions: air carrier flow rate, 200 mL min<sup>-1</sup>; CO gas volume at atmosphere pressure, 3 × 50 mL; temperature, at about 160 °C.

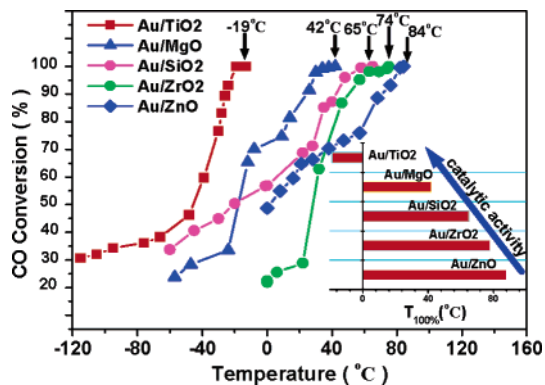


**Figure 2.** Curves of CO conversion as a function of temperature for different oxide-supported gold catalysts. Reaction conditions: 0.05 g of catalyst, 3.99% CO in dry air at a total flow rate of 80 mL min<sup>-1</sup>. Inset: Temperature of 100% conversion of CO oxidation for these gold catalysts. Catalytic activities ranked in the order of Au/TiO<sub>2</sub> > Au/MgO > Au/SiO<sub>2</sub> > Au/ZrO<sub>2</sub> > Au/ZnO.

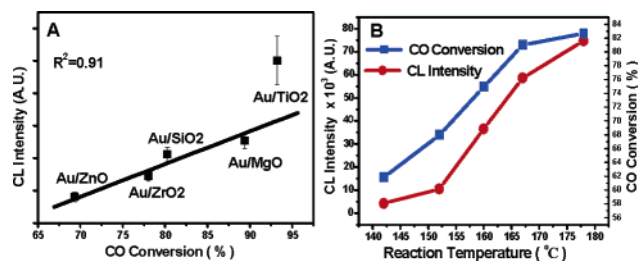


**Figure 3.** Correlation of CL intensities with CO conversions for each gold catalyst (A) and at a series of reaction temperatures for the Au/ZnO catalyst (B).

with these supported gold catalysts on a ceramic chip with a temperature controller. When the catalytic CO oxidation occurs, the CL on each spot of the array is imaged simultaneously on monochromatic film (Figure 4). The brightest spot corresponds to Au/TiO<sub>2</sub>, whereas the weakest one corresponds to Au/ZnO. The brightness of the image is consistent with the catalytic activities of these catalysts. The brightness of the CL image increases with an increase of CO gas and reaction temperatures (Figure S6). Thus, a qualitative overview of catalytic activities of these gold catalysts at different conditions can be achieved by the CL-based array imaging according to the brightness. It should be noted that the present method is effective for judging activity, while possibly insufficient for judging selectivity.

In summary, we have developed a new CL-based imaging method, which indicated the feasibility of a simple, rapid, and parallel screening for the catalytic activity of a catalyst based on the good correlation between the CL intensity and the CO

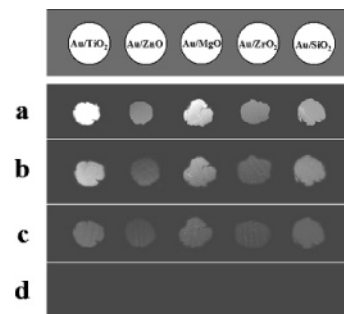


**Figure 4.** The CL-based array imaging photographs at the same reaction temperature of about 160 °C following a change of CO gas amount (a) 8 × 50 mL; (b) 4 × 50 mL; (c) 2 × 50 mL; (d) without CO injection. On the basis of the brightness, an order is followed as Au/TiO<sub>2</sub> > Au/MgO > Au/SiO<sub>2</sub> > Au/ZrO<sub>2</sub> > Au/ZnO.

conversion. This technique would be potentially applied to explore new species of catalysts synthesized by combinatorial approaches.

**Acknowledgment.** The work is supported financially by the National Natural Science Foundation of China (Nos. 20535020, 20635002, and 20575034).

**Supporting Information Available:** Detailed experiment procedures, TEM images of gold catalysts, CL features of CO oxidation, and CL images of reaction under different temperatures. This material is available free of charge via the Internet at <http://pubs.acs.org>.

## References

- (1) Haruta, M.; Tsubota, S.; Kobayashi, T.; Kageyama, H.; Genet, M. J.; Delmon, B. *J. Catal.* **1993**, *144*, 175.
- (2) Yan, W.; Brown, S.; Pan, Z.; Mahurin, S.; Overbury, S.; Dai, S. *Angew. Chem., Int. Ed.* **2006**, *45*, 3614.
- (3) Yan, W.; Mahurin, S. M.; Pan, Z.; Overbury, S. H.; Dai, S. *J. Am. Chem. Soc.* **2005**, *127*, 10481.
- (4) Comotti, M.; Li, W. C.; Spliethoff, B.; Schuth, F. *J. Am. Chem. Soc.* **2006**, *128*, 917.
- (5) Mohr, C.; Hofmeister, H.; Radnik, J.; Claus, P. *J. Am. Chem. Soc.* **2003**, *125*, 1905.
- (6) Lang, H.; Maldonado, S.; Stevenson, K. J.; Chandler, B. D. *J. Am. Chem. Soc.* **2004**, *126*, 12949.
- (7) Yoon, B.; Hakkinen, H.; Landman, U.; Worz, A. S.; Antonietti, J. M.; Abbet, S.; Judai, K.; Heiz, U. *Science* **2005**, *307*, 403.
- (8) Chen, M.; Kumar, D.; Yi, C.; Goodman, D. W. *Science* **2005**, *310*, 291.
- (9) Holzwarth, A.; Schmidt, H. W.; Maier, W. *Angew. Chem., Int. Ed.* **1998**, *37*, 2644.
- (10) (a) Su, H.; Yeung, E. S. *J. Am. Chem. Soc.* **2000**, *122*, 7422. (b) Su, H.; Hou, Y.; Hou, R. S.; Shrader, G. L.; Yeung, E. S. *Anal. Chem.* **2001**, *73*, 4434.
- (11) Wahler, D.; Badalassi, F.; Crotti, P.; Reymond, J. L. *Angew. Chem., Int. Ed.* **2001**, *40*, 4457.
- (12) Senkan, S. M. *Nature* **1998**, *394*, 350.
- (13) Breyse, M.; Claudel, B.; Faure, L.; Guenin, M.; Williams, R. J. *J. Catal.* **1976**, *45*, 137.
- (14) (a) Nakao, K.; Ito, S.; Tomishige, K.; Kunimori, K. *J. Phys. Chem. B* **2005**, *109*, 17553. (b) Nakao, K.; Ito, S.; Tomishige, K.; Kunimori, K. *J. Phys. Chem. B* **2005**, *109*, 24002.
- (15) Okabayashi, T.; Fujimoto, T.; Yamamoto, I.; Utsunomiya, K.; Wada, T.; Yamashita, Y.; Nakagawa, M. *Sens. Actuators B* **2000**, *64*, 54.
- (16) (a) Na, N.; Zhang, S.; Wang, S.; Zhang, X. *J. Am. Chem. Soc.* **2006**, *128*, 14420. (b) Sun, Z.; Yuan, H.; Liu, Z.; Han, B.; Zhang, X. *Adv. Mater.* **2005**, *17*, 2993. (c) Ye, Q.; Gao, Q.; Zhang, X.; Xu, B. *Catal. Commun.* **2006**, *7*, 589. (d) Lv, Y.; Zhang, S.; Liu, G.; Huang, M.; Zhang, X. *Anal. Chem.* **2005**, *77*, 1518. (e) Huang, G.; Lv, Y.; Zhang, S.; Yang, C.; Zhang, X. *Anal. Chem.* **2005**, *77*, 7356. (f) Zhu, Y.; Shi, J.; Zhang, Z.; Zhang, C.; Zhang, X. *Anal. Chem.* **2002**, *74*, 120. (g) Liu, G.; Zhu, Y.; Zhang, X.; Xu, B. *Anal. Chem.* **2002**, *74*, 6279.

JA0702768